Available online at www.sciencedirect.com
ScienceDirect
Thermochimica Acta 449 (2006) 55–60
thermochimica acta
www.elsevier.com/locate/tca

Thermal decomposition of some copper–iron polynuclear coordination compounds containing glycine as ligand, precursors of copper ferrite

Oana Carp *, Dana Gingasu, Ioana Mindru, Luminita Patron

Institute of Physical Chemistry, Splaiul Independentei 202, Sector 6, Bucharest, Romania

Received 16 August 2005; received in revised form 28 June 2006; accepted 15 July 2006
Available online 5 August 2006

Abstract

The thermal behaviour of three coordination compounds, precursors of copper ferrite, namely $[Fe_2Cu(NH_2CH_2COOH)_{4.5}](NO_3)_8{\cdot}4H_2O$ (I), $[Fe_2Cu(NH_2CH_2COO)_4(OH)_3](NO_3){\cdot}H_2O$ (II) and $[Fe_2Cu(NH_2CH_2COO)_6(NH_2CH_2COOH)_2](NO_3)_2$ (III), has been investigated. For a complete and reliable assignment of the thermal transformations, the isolable intermediates and end products were characterized by IR and X-ray diffraction. The coordination compounds which undergo a stepwise decomposition in the temperature range 60–375 °C are less stable than free glycine (206–375 °C), indicating the occurrence of some self-propagating reactions. The nitrate/glycine ratio contained by the parent coordination compound, affects the final decomposition temperature (decreases as the ratio increases) but not the decomposition mechanism, and the mean particles size of the decomposition end product Fe_2CuO_4 (an optimum value has to be found in order to avoid local combustion occurrences).

Keywords: Copper ferrite; Copper iron coordination compound; Self-propagating reaction

1. Introduction

In the last decade the use of polynuclear compounds as source of oxides with various structures (spinelic [1–11], garnet [12,13], hexagonal [14,15] and perovskitic [16–20]) has expanded. The use of the thermal decomposition of polynuclear coordination precursors in the synthesis of oxides is considered as an efficient method due to the valuable benefits [21–23] related to the:

- synthesis reproducibility;
- accessibility (the most raw materials have moderate costs);
- diversity of metallic ions combinations (a variety of cations and versatile combinations ratios);
- homogeneity of the mixed oxides (the metallic cations are build up on an atomic scale in an ordered precursor and during the thermal decomposition the uniform distribution is largely retained);
- oxides particles with sizes lower than 500 Å, inferior, than those obtained through conventional or other non-conventional synthesis methods, due to low decomposition temperatures (often mixed oxide lattice is already available at the decomposition completion).

Although, no systematically studies concerning the influence of the composition and architecture of precursors on the size of particles are made, several trends are to be mentioned. Low decomposition temperatures lead to fine particles. Thus, the use of ligands which volatilize or decompose to volatile compounds at low temperatures, represents an indispensable requirement for nanosized synthesis of mixed oxides. Therefore, the thermal decomposition of carboxylates complexes (mono, poly and hydroxy) has been exploit in order to obtain of mixed oxides. On the other hand, the evolving of a large amount of gases in a short lapse of time may represent a significant parameter in the synthesis of nanosized oxides. A beneficial choice in order to fulfill this demand is the presence in the parent coordination compound of both oxidizing and reducing components, which, during their simultaneous evolving interact, producing a large amount of gases. Coordination compounds containing as ligand urea (reducing agent), and nitrate anion as outer sphere ion (oxidant agent), are quite a suitable type of precursors [24–27]. Nevertheless, the use as ligand of urea has the disadvantage, of a lower coordination ability comparative with carboxylates ligands. That is why, we consider that a next step of the

* Corresponding author. Fax: +4021 3121147.
E-mail address: carp@apia.ro (O. Carp).

0040-6031/$ – see front matter © 2006 Elsevier B.V. All rights reserved.
doi:10.1016/j.tca.2006.07.023

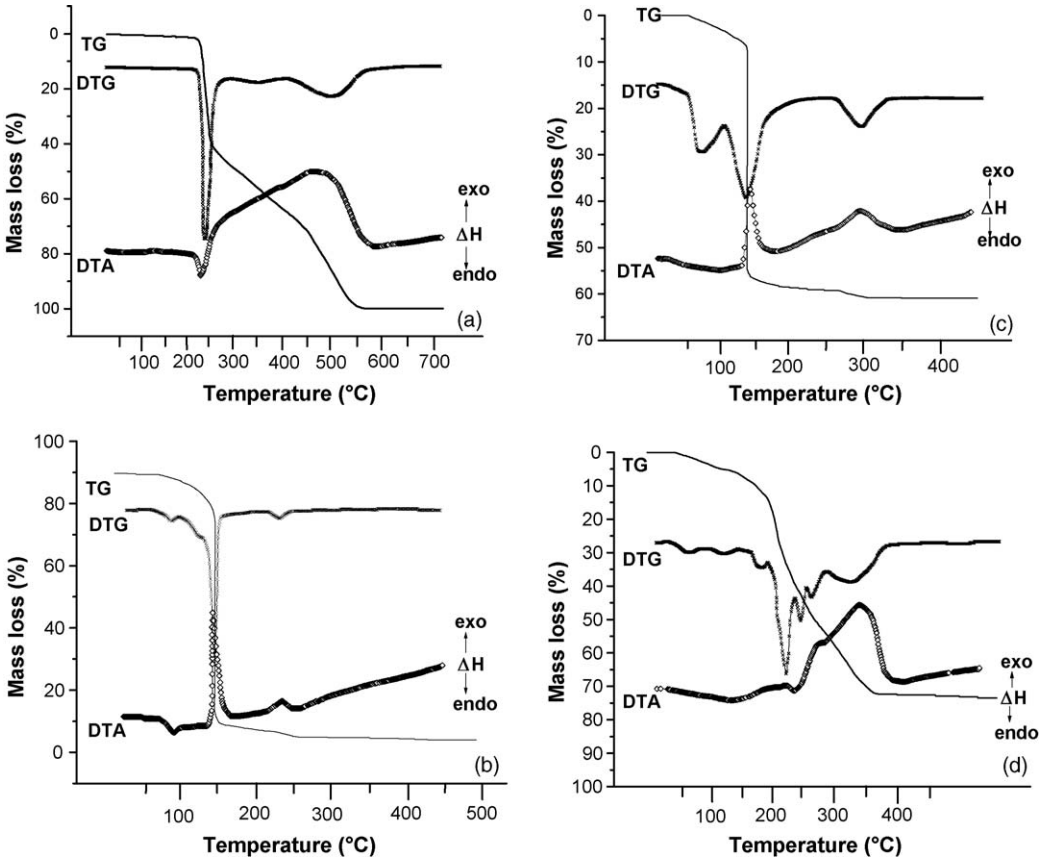

Fig. 1. TG, DTG and DTA curves of the: (a) glycine; (b) $[Fe_2Cu(NH_2CH_2COOH)_{4.5}](NO_3)_8{\cdot}4H_2O$ (I); (c) $[Fe_2Cu(NH_2CH_2COO)_4(OH)_3](NO_3){\cdot}1H_2O$ (II); (d) $[Fe_2Cu(NH_2CH_2COO)_6(NH_2CH_2COOH)_2](NO_3)_2$ (III).

research in this topic, is to find a ligand which joins the good coordination ability of a carboxylic acid and the reducing characteristics of urea, amino acids representing a good choice. As starting point, the first representative of this class, glycine (aminoacetic acid, NH_2CH_2COOH), is used in the present paper as ligand in coordination compounds precursors of copper ferrite, namely $[Fe_2Cu(NH_2CH_2COOH)_{4.5}](NO_3)_8{\cdot}4H_2O$ (I), $[Fe_2Cu(NH_2CH_2COO)_4(OH)_3](NO_3){\cdot}1H_2O$ (II) and $[Fe_2Cu(NH_2CH_2COO)_6(NH_2CH_2COOH)_2](NO_3)_2$ (III).

2. Experimental

The synthesis method and characterization of the three investigated polynuclear coordination compounds $[Fe_2Cu(NH_2CH_2COOH)_{4.5}](NO_3)_8{\cdot}4H_2O$ (I), $[Fe_2Cu(NH_2CH_2COO)_4(OH)_3](NO_3){\cdot}H_2O$ (II) and $[Fe_2Cu(NH_2CH_2COO)_6(NH_2CH_2COOH)_2](NO_3)_2$ (III) is reported elsewhere [28]. It is worth to mention, that iron cations (Fe^{3+}, d^5) are present in an octahedral high spin configuration in all three coordination compounds, while copper ions (Cu^{2+}, d^9) adopt different configurations in the investigated compounds: a pseudooctahedral (in coordination compounds (I) and (III)) and pseudotetrahedral (in coordination compound (II)).

The thermal measurements (TG, DTG and DTA) were performed using a Q–1500 D Paulik–Paulik–Erdey derivatograph in a static air atmosphere, at heating rates in the range 2.5–5 K min^{-1}. FTIR spectra (400–4000 cm^{-1}) were recorded with a BIO-RAD FTIR 125 type spectrophotometer in KBr pellets. The XRD analysis was performed on a Rigaku-Multiflex diffractometer, using Cu Kα. For quantitative analysis a step scanning technique was applied in the 2θ range 20–80 with a step of 2° min^{-1}. For the determination of the average crystallites size it has been used the Scherrer formula $D = [0.91\,\lambda/(\beta\cos\theta)]57.32$, where D is the crystallite size, λ the wave length (Cu Kα), β the corrected half-width obtained using α-quartz as reference and the Warren formula and θ is the diffraction angle of the first 10 more intensive diffraction peaks.

3. Results

The thermal decomposition curves (TG, DTG and DTA) of the three coordination compounds and glycine (registered for comparison) are depicted in Fig. 1.

Glycine decomposes through three steps (Fig. 1(a)), one accompanied by a sharp endothermic effect and the other two associated with exothermic ones. The decomposition stoichiometries (in accordance with some MS data [29] and our FTIR investigations, Fig. 2), correspond to:

(i) in the temperature range 206–290 °C ($T_{max\ DTG}$ = 239 °C) simultaneous melting and evolving of a H_2O and NH_3 molecule (calcd./found: 46.66/46.05%). It is known that

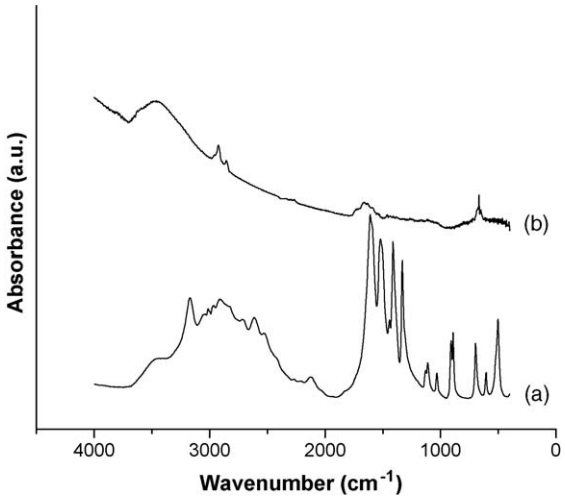

Fig. 2. IR spectra pf glycine (a) and the intermediate obtained after the first decomposition reaction (b).

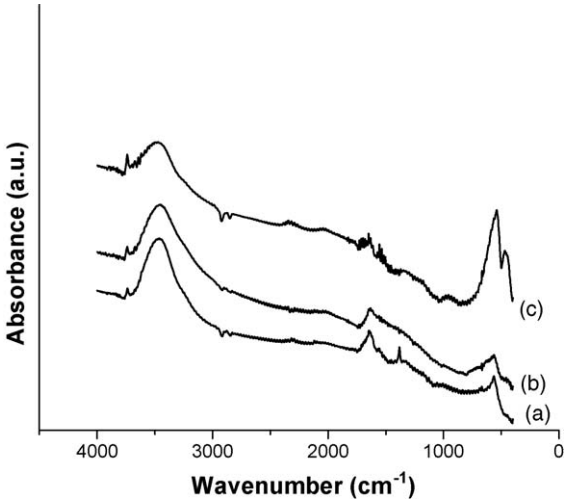

Fig. 3. IR spectra of the decomposition intermediates obtained from the $[Fe_2Cu(NH_2CH_2COOH)_{4.5}](NO_3)_8{\cdot}4H_2O$ (I) coordination compound (a) after the second decomposition step; (b) after the third decomposition step; (c) after the fourth decomposition step.

amino acids do not exhibit clean melting points, and during their melting they decompose into lower mass compounds. The NH_3 evolving is confirmed by the disappearance of FTIR characteristics bands (3170 (νNH_2), 1517 ($\delta_{sim}NH_3^+$), 1111 ($\rho_r NH_3$), 1033 ($\nu_{as}CCN$) and 892 ($\nu_{sim}CCN$) cm^{-1}). Beside the conservation of the carbonyl group (broad band at ∼1660 ($\nu_{as}COO$ and $\nu_{sim}COO$) and 668 (δCOO) cm^{-1}), typical bands of aliphatic $-CH_2-$ (2924($\nu_{as}CH_2$), 2856($\nu_{sim}CH_2$) cm^{-1}) develop (Fig. 2(b)). Formation of glycine condensation products may be responsible for this decomposition step;

(ii) in the temperature range 290–410 °C removal of a water molecule ($T_{max\ DTG}$ = 350 °C);

(iii) removal of two CO_2 molecules in the temperature range 410–589 °C ($T_{max\ DTG}$ = 511 °C).

The studied complexes, which undergo in the temperature range 60–375 °C a stepwise decomposition are less stable than the free ligand. This behaviour is contrary with the usual one, respective a higher thermal stability of the ligand introduced into complexes (due to its coordination) comparative with corresponding free ligand [30–35]. The lower thermal stability expressed by complexes than the free ligand, indicates or a catalytic effect introduced by the metallic cation [36–38], or, the occurrence of some self-propagating reactions [26–28].

The first polynuclear coordination compound $[Fe_2Cu(NH_2CH_2COOH)_{4.5}](NO_3)_8{\cdot}4H_2O$ (I), underwent four-step decomposition (Fig. 1 (b)) in the temperature range 62–292 °C. The observed mass loss (78.01%) is in good agreement with the calculated one (77.86%), considering as end product copper ferrite (Fe_2CuO_4). The first two decomposition steps (62–98 °C, $T_{max\ DTG}$ = 80 °C, and 98–139 °C, $T_{max\ DTG}$ = 121 °C) associated with endothermic effects correspond to the evolving of one water molecule (calcd./found: 1.67/1.79%), respective three water molecules (calcd./found: 5.01/4.88%). The next decomposition stage (139–174 °C, $T_{max\ DTG}$ = 158 °C), is a fast and intensive exothermic process, consisting in simultaneous evolving of NO_3^- and glycine ligand. Simultaneously, glycine is oxidized by nitrate anions (resulting carbon dioxide, nitrogen, nitrogen dioxide and water [39]). Based on thermogravimetric calculations (68.15% loss) and FTIR investigations of the isolated intermediate (Fig. 3(a)), the formation of an aqua-hydroxo complex of molecular formula $[Fe_2Cu(H_2O)_x(OH)_y]O_{4-0.5y}$ with $x + y = 2$ is stipulated (3737, ∼3462 (O–H stretching) and 1641 cm^{-1} (O–H bending)). The formation of this aqua-hydroxo species may be explained as follows: during the last decomposition step, a highly reactive solid residue forms, reacting with water generated during the redox reaction of glycine with NO_3^-. Next (174–240 °C), a continuous weight loss (1.59%) representing the formation of an aqua-hydroxo complex with $x + y = 1$ is registered (Fig. 3(b)). On further heating, in the temperature range (240–292 °C, $T_{max\ DTG}$ = 261 °C) the aqua-hydroxo complex decomposes through an exothermic step to copper ferrite (weight loss of 1.60%). The exothermicity of this process may be related to some structural rearrangements of the lattice, namely the formation of spinel lattice. Although the XRD analysis evidences an amorphous material, the FTIR spectra of the decomposition end product (Fig. 2(c)) shows the absorption bands at 541 and 467 cm^{-1} characteristic to the intrinsic vibrations of the tetrahedral and respective octahedral groups of the spinel lattice [40]. A calcination treatment of 1 h at 800 °C lead to the formation of a copper ferrite (Fe_2CuO_4) with mean particles size of 240 Å accompanied by small quantities of CuO and α-Fe_2O_3 (Fig. 4(a)).

The coordination compound $[Fe_2Cu(NH_2CH_2COO)_4(OH)_3](NO_3){\cdot}H_2O$ (II) decomposes in the temperature range 50–375 °C through three stages (Fig. 1(c)). The observed mass loss, 60.88%, confirms the formation as an end decomposition product of a compound with molecular formula Fe_2CuO_4 (theoretical mass loss 60.27%). A first endothermic step (50–110 °C, $T_{max\ DTG}$ = 61 °C), corresponds to the evolving of the water molecule (calcd./found: 2.98/3.38%). The second one, is a fast, strong exothermic process (110–141 °C, $T_{max\ DTG}$ = 138 °C),

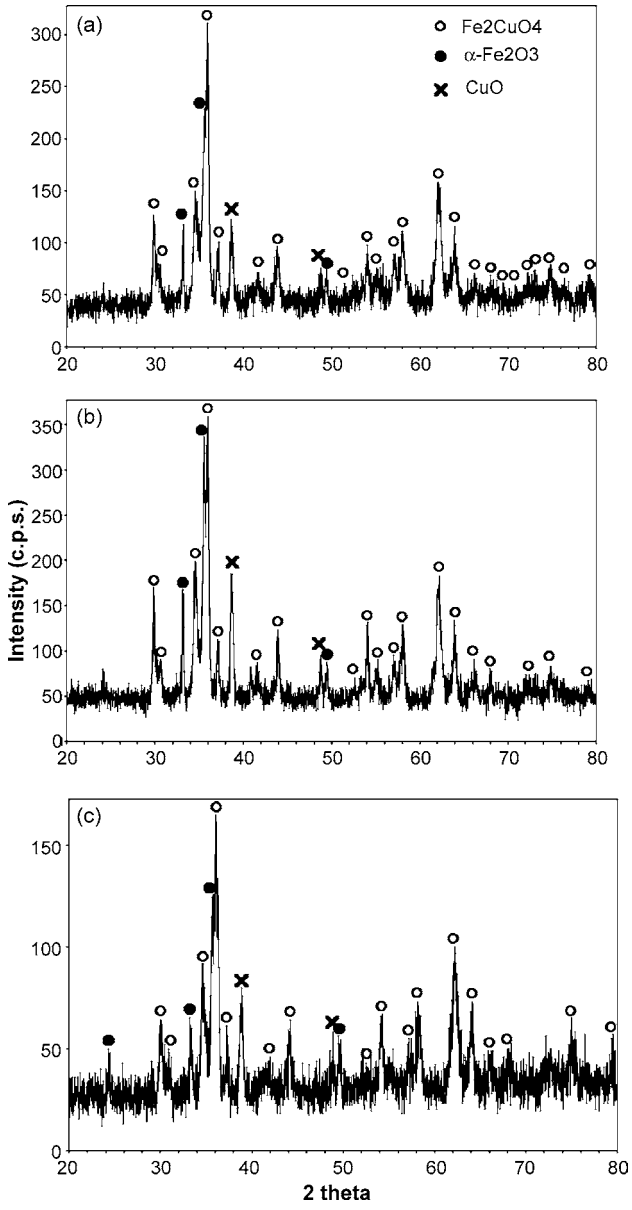

Fig. 4. X-ray diffraction patterns of the oxides obtained after a heating treatment of 1 h at 800 °C; (a) oxides derived from precursor $[Fe_2Cu(NH_2CH_2COOH)_{4.5}](NO_3)_8{\cdot}4H_2O$ (I); (b) oxides derived from precursor $[Fe_2Cu(NH_2CH_2COO)_4(OH)_3](NO_3){\cdot}1H_2O$ (II); (c) oxides derived from precursor $[Fe_2Cu(NH_2CH_2COO)_6(NH_2CH_2COOH)_2](NO_3)_2$ (III).

consisting in the evolving of NO^-_3 and HO^- anions and, degradative oxidation of the glycine ligand. Similar to the first coordination compound an aqua-hydroxo complex of molecular formula $[Fe_2Cu(H_2O)_x(OH)_y]O_{4-0.5y}$ with $x+y=1$ is expected to be formed. The weight loss (55.26%) and the registered FTIR frequencies (3775, ~3460 (O–H stretching) and 1640 cm^{-1}(O–H bending)) of the intermediate sustain this affirmation. The intermediate is stable in the temperature range 141–251 °C, whereupon it decomposes (251–375 °C, $T_{max\ DTG}$ = 310 °C) through an exothermic process to a compound corresponding to molecular formula of copper ferrite (mass loss 2.44%). Similar to the first compound, the exothermicity of this later step may be related to some structural

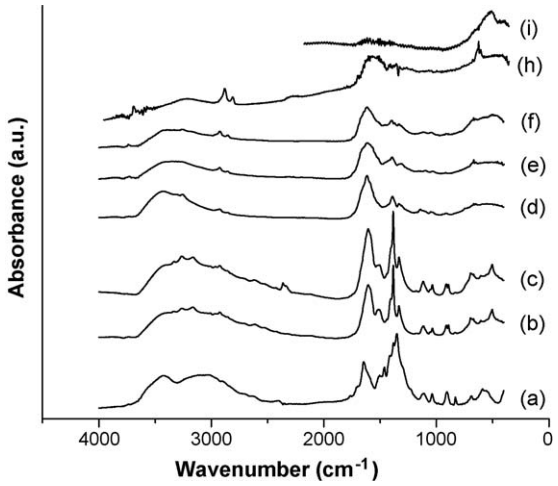

Fig. 5. IR spectra of the $[Fe_2Cu(NH_2CH_2COO)_4(OH)_3](NO_3){\cdot}1H_2O$ (II) coordination compound and its decomposition intermediates; (a) coordination compound; (b) after the first decomposition step; (c) after the second decomposition step; (d) after the third decomposition step; (e) after the fourth decomposition step; (f) after the fifth decomposition step; (g) after the sixth decomposition step; (h) after the seventh decomposition step.

rearrangements of the lattice. XRD and FTIR investigations led to the same findings as for the first compound (XRD amorphous and specific FTIR frequencies at 560 and 462 $cm^{-1}$of the spinel lattice). A calcination of 1 h at 800 °C determines the formation of copper ferrite with mean particles size of 180 Å (Fig. 4(b)). The lower value of this parameter comparative with the one obtained for the first compound is decided by the lower exothermicity of the redox reaction NO_3^-/glycine (compound (I)/compound (II) = 1.77/0.25). As in the first case, impurities of CuO and α-Fe_2O_3 are also identified.

The third compound $[Fe_2Cu(NH_2CH_2COO)_6(NH_2CH_2COOH)_2](NO_3)_2$ (III) suffers a seven stage decomposition in the temperature range 55–380 °C (Fig. 1(d)). The experimental weight loss assuming Fe_2CuO_4 formation, shows agreement with theoretical weight loss (calcd./found: 73.21/73.52%). The first two endothermic decomposition steps (55–80 °C, $T_{max\ DTG}$ = 62 °C and 80–131 °C, $T_{max\ DTG}$ = 105 °C) represent the evolving in each one of a water molecule (calcd./found: 2.01/2.18% and 2.01/3.06%). The analysis of FTIR spectrum (Fig. 5(b and c)) reveals three interesting results: (a) the appearance of bands characteristic to free glycine: ~3400 and 3166 cm^{-1} (νNH_2 as and sim), the shift to lower wave numbers of $\nu_{as}CO$ band (1646 → 1607 cm^{-1}) and the splitting of the band from 906 cm^{-1} into two bands at 911 and 892 cm^{-1} (νCCN); (b) the decrease of the bands characteristic to NH_2 from 3419 to ~3100 cm^{-1} (νNH_2 as and sim) comparative to the initial coordination compound; (c) the appearance of the band characteristic to secondary amide at 1332 cm^{-1} (corresponding to the νCN–δNH vibrations). Obviously, due to the overlapping, it is not possible to discriminate several characteristics bands of the mentioned compounds. Considering the above findings the following mechanism for these two steps may be advanced: during the heating, the supplied energy determines a detachment of the neutral glycine ligand (through the breaking of the coordination bonds) from the coordination com-

pound. The detached glycine suffers further an internal dehydration, leading to an cyclic amide [41]. The next decomposition stage, which occurs in the temperature range 131–178 °C ($T_{max\ DTG}$ = 170 °C), represents the evolving of NO_3^-. Due to the oxidizing atmosphere determined by NO_3^- anions evolving, a transformation of the glycine anion ligands to hydroxyacetate anion (HO–CH_2–COO^-) takes place. The proposed intermediate is formulated as [$Fe_2Cu(HOCH_2COO)_8$]. The concordance of the theoretical and experimental mass loss (calcd./found: 13.21/11.28%), the disappearance of the strong ν_{as} band corresponding to NO_3^- (1383 cm^{-1}), the development of characteristic bands of C–OH group (∼3500 (νOH) and 1142 cm^{-1} (νC–OH) cm^{-1}) and, the preservation of the distinctive bands of aliphatic –CH_2– (2829($\nu_{as}CH_2$), 2855($\nu_{sim}CH_2$), the doublet at 1121–1048 cm^{-1} (δCH_2)) and C–C (913 cm^{-1} (νC–C)) supports this affirmation (Fig. 5(d)). The next four steps (178–220, 220–240, 240–275 and 275–380 °C with $T_{max\ DTG}$ = 198, 230, 250 and 330 °C), are rather complicated being impossible an accurate assignation of the decomposition intermediates. The FTIR investigations evidence besides the maintenance of the COO, –CH_2– and C–C groups until the last process, the appearance of bands characteristic to aqua-hydroxo species (∼3730 cm^{-1}, corresponding to O–H stretching modes during the fourth step and ∼1600 cm^{-1}, assigned to O–H bending mode during the last stage of decomposition, Fig. 5(e–h)). The mentioned findings lead to following assumptions concerning the decomposition which occurs this temperature range: water may be evolved from the acid, being know that α-hydroxy acids eliminate easy water during heating. In consequence, the formation of both polycondensation and aqua-hydroxo intermediates may be advanced. The spinel specific absorption bands (558 and 442 cm^{-1}) are formed during the last decomposition step. After a calcination treatment of 1 h at 800 °C a Fe_2CuO_4 with mean particles sizes of 290 Å is obtained (Fig. 4(c)). Impurities of CuO and α-Fe_2O_3 are also detected.

4. Conclusions

The three studied coordination compounds [$Fe_2Cu(NH_2CH_2COO)_{4.5}$]$(NO_3)_8 \cdot 4H_2O$ (I), [$Fe_2Cu(NH_2CH_2COOH)_4(OH)_3$]$(NO_3)$ (II) and [$Fe_2Cu(NH_2CH_2COO)_6(NH_2CH_2COOH)_2$]$(NO_3)_2$ (III), decompose at lower temperatures comparative with the free glycine ligand, leading to end products in which the spinel lattice is already available. The main controllable processing variable is the glycine to nitrate ratio, which affects both the final decomposition temperature (but not the decomposition mechanism) and the values of particles size of the Fe_2CuO_4:

	Compound		
	(I)	(II)	(III)
NO_3^-/glycine	1.77	0.25	0.25
Final decomposition temperature (°C)	292	375	375
Fe_2CuO_4 mean particles size (Å) (1 h, 800 °C)	240	180	290

The profiles of the thermogravimetric curves of the [$Fe_2Cu(NH_2CH_2COOH)_{4.5}$]$(NO_3)_8 \cdot 4H_2O$ (I) and [$Fe_2Cu(NH_2CH_2COO)_4(OH)_3$]$(NO_3) \cdot H_2O$ (II) polynuclear coordination compounds are similar. The decomposition occurs through three/four decomposition steps: one/two endothermic process(es) corresponding to water elimination, followed by two exothermic steps corresponding to NO_3^- and glycine anions evolving, with formation of aqua-hydroxo species as intermediates. The considerable differences in composition, is reflected in the temperature ranges of thermal decomposition occurrence of the third process (temperatures higher with about 85 °C being registered for the first compound). On the other hand, a gradual decomposition through seven steps is recorded for the [$Fe_2Cu(NH_2CH_2COO)_6(NH_2CH_2COOH)_2$]$(NO_3)_2$ polynuclear compound.

References

[1] G. Marinescu, L. Patron, O. Carp, L. Diamandescu, N. Stanica, A. Meghea, M. Brezeanu, J.C. Grenier, J. Etourneau, J. Mater. Chem. 12 (2002) 3458–3462.
[2] O. Carp, L. Patron, I. Mindru, G. Marinescu, L. Diamandescu, A. Banuta, J. Therm. Anal. Calorim. 74 (2003) 789–799.
[3] P.D. Thang, G. Rijnders, D.H.A. Blank, J. Magn. Magn. Mater. 295 (2005) 251–256.
[4] F. Kenfack, H. Langbein, Thermochim. Acta 426 (2005) 61–72.
[5] S.M. Montemayor, L.A. Garcia-Cerda, J.R. Torres-Libián, Mater. Lett. 59 (2005) 1056–1060.
[6] A.K. Nikumbh, A.V. Nagawade, G.S. Gugale, M.G. Chaskar, P.P. Bakare, J. Mater. Sci. 37 (2001) 637–647.
[7] P. Sainamthip, V.R.W. Amarakoon, J. Am. Ceram. Soc. 71 (1988) C92–C96.
[8] Z. Yue, J. Zhou, L. Li, Z. Giu, J. Magn. Magn. Mater. 233 (2001) 224–229.
[9] A. Verma, T.C. Goel, R.G. Mendiratta, R.G. Gupta, J. Magn. Magn. Mater. 192 (1999) 271–276.
[10] M. Moullem-Bahout, S. Bertrand, O. Peňa, J. Solid State Chem. 178 (2005) 1080–1086.
[11] A.K. Singh, A.K. Singh, T.C. Goel, R.G. Mendiratta, J. Magn. Magn. Mater. 281 (2004) 276–280.
[12] P. Spacu, S. Plostinaru, L. Patron, Roum. Chem. Q. Rev. 1 (1993) 119–136.
[13] P. Vaqueiro, M.A. López, Chem. Mater. 9 (1997) 2836.
[14] O. Carp, L. Patron, E. Segal, R. Barjega, M. Brezeanu, J. Therm. Anal. Calorim. 56 (1999) 513–518.
[15] T. Ogasawara, N.A.S. Oliveira, J. Magn. Magn. Mater. 217 (2000) 147–154.
[16] O. Carp, L. Patron, A. Ianculescu, J. Pasuk, R. Olar, J. Alloys Compd. 351 (2003) 314–318.
[17] O. Carp, L. Patron, A. Ianculescu, D. Crisan, N. Dragoe, R. Olar, J. Therm. Anal. Calorim. 72 (2003) 253–261.
[18] P.K. Gallagher, Mater. Res. Bull. 3 (1968) 225–232.
[19] Y. Masuda, Y. Seto, X. Wang, Y. Yukawa, T. Arii, J. Therm. Anal. Calorim. 60 (2000) 1033–1041.
[20] R.N. Basu, F. Tietz, E. Wessel, H.P. Buchkremer, D. Stöver, Mater. Res. Bull. 39 (2004) 1335–1345.
[21] L. Patron, I. Mindru, G. Marinescu, Magnetic nanomaterials: nonconventional synthesis and chemical design, in: Dekker Encyclopedia of Nanoscience and Nanotechnology, 2004, pp. 1683–1699.
[22] I. Mindru, L. Patron, M. Brezeanu, Roum. Chem. Q. Rev. 4 (3–4) (1996) 167–181.
[23] O. Carp, Rev. Roum. Chem. 46 (11) (2001) 1189–1202.
[24] O. Carp, L. Patron, M. Brezeanu, J. Therm. Anal. Calorim. 56 (1999) 561–568.
[25] O. Carp, L. Patron, A. Reller, J. Therm. Anal. Calorim. 73 (2003) 867–876.
[26] O. Carp, L. Patron, L. Diamandescu, A. Reller, Thermochim. Acta 390 (2002) 169–177.
[27] R. Kalai Selvan, C.O. Augustin, L. John Berchmans, R. Saraswathi, Mater. Res. Bull. 38 (2003) 41–54.

[28] D. Gingasu, I. Mindru, L. Patron, O. Carp, N. Stanica, I. Balint, J. Eur. Ceram. Soc., in press.
[29] R. Mrozek, Z. Rzączyńska, M. Sikorska-Iwan, J. Therm. Anal. Calorim. 63 (2001) 839–846.
[30] M. Sikorska-Iwan, R. Mrozek, Z. Rzączyńska, J. Therm. Anal. Calorim. 60 (2000) 139–144.
[31] S.B. Jagtap, R.C. Chikate, O.S. Yemul, R.S. Ghadage, B.A. Kulkarni, J. Therm. Anal. Calorim. 78 (2004) 251–262.
[32] R.R. Mahajan, P.S. Makashir, J.P. Agrawal, J. Therm. Anal. Calorim. 65 (2001) 935–942.
[33] I.M.M. Kenawy, M.A. Hafez, R.R. Lashein, J. Therm. Anal. Calorim. 65 (2001) 723–736.
[34] K. Mészáros Szécsény, V.M. Leovac, Ž.K. Jaćimović, G. Pokol, J. Therm. Anal. Calorim. 74 (2003) 943–952.
[35] B.N. Sivasankar, L. Ragunath, Thermochim. Acta 397 (2003) 237–247.
[36] A.S. Zidan, A.I. El-Said, M.S. El-Meligy, A.A.M. Aly, O.F. Mohammed, J. Therm. Anal. Calorim. 62 (2000) 665–679.
[37] K. Andjelković, M. Šumar, I. Ivanović-Burmazović, J. Therm. Anal. Calorim. 66 (2001) 759–778.
[38] M. Badea, R. Olar, E. Cristurean, D. Marinescu, A. Emandi, P. Budrugeac, E. Segal, J. Therm. Anal. Calorim. 77 (2004) 815–824.
[39] C.H. Yan, Z.G. Xu, F.X. Xheng, Z.M. Wang, L.D. Sun, C.S. Liao, J.T. Jia, Solid State Commun. 111 (1999) 287–291.
[40] R. Kalai Selvan, C.O. Augustin, L.J. Berchmans, R. Saraswathi, Mater. Res. Bull. 38 (2003) 41–54.
[41] C.D. Nenitescu, Organic Chemistry, vol. II, VIIIth ed., Didactics and Pedagocical Printing House, Bucharest, 1980, p. 375, (in Romanian).